ONLINE FIRST

This is a provisional PDF only. Copyedited and fully formatted version will be made available soon.

ISSN: 0015-5659

e-ISSN: 1644-3284

Volumetric analysis of the cranial and nasal cavity from micro-computed tomography scans in the rabbit

Authors: Caner Bakıcı, Remzı Orkun Akgun, Okan Ekım, Cıgdem Soydal, Cagdas Oto

DOI: 10.5603/FM.a2019.0073

Article type: ORIGINAL ARTICLES

Submitted: 2019-05-10

Accepted: 2019-06-21

Published online: 2019-07-02

Volumetric analysis of the cranial and nasal cavity from micro-computed tomography scans in the rabbit

Volume analysis of rabbit nasal cavity

Caner Bakıcı[1], Remzı Orkun Akgun[1], Okan Ekım[1], Cıgdem Soydal[2], Cagdas Oto[1]

[1]Ankara University, Faculty of Veterinary Medicine, Department of Anatomy, Ziraat District, Şehit Ömer Halisdemir blvd, Altindag, 06110 Ankara, Turkey

[2]Ankara University, School of Medicine, Department of Nuclear Medicine, Cebeci Hospital, 06590 Ankara, Turkey

Address for correspondence: Caner BAKICI, Ankara University, Faculty of Veterinary Medicine, Department of Anatomy, Ziraat District, Şehit Ömer Halisdemir blvd, Altindag, 06110 Ankara, Turkey, e-mail: vetcanerbakici@gmail.com

ABSTRACT

Background: The aim of the study was to estimate the volume values of the cranial cavity and nasal cavity structures and to compare the efficiency of manual segmentation of three dimensional (3D) reconstruction and Cavalieri's principle (CP) methodologies.

Materials and methods: Volume values of the cranial cavity (CC), maxillary sinus (MS), dorsal conchal sinus (DCS), dorsal nasal meatus (DNM), middle nasal meatus (MNM), ventral nasal meatus (VNM), ventral nasal concha (VNC), middle nasal concha (MNC) and nasal vestibule (NV) were estimated with manual segmentation and Cavalieri's principle from micro-computed tomography (μCT) images in five male New Zealand white rabbits. Volume measurements and elapsed time were compared with each other. 3D reconstruction models of nasal and cranial cavity structures were created.

Results: There was a statistically significant difference between methods of the MS, DCS, DNM, MNM, VNM, VNC, and MNC volume measurements. Additionally, there was a statistically significant difference between the volumetric analysis time period of the methods and Cavalieri's principle was found much shorter than manual segmentation.

Conclusions: Realistic results were achieved in a short time with the Cavalieri principle among the Stereology methods. It is thought that these image and quantitative data results can be used for modeling, toxicology and pathology studies such as acute and chronic rhinitis or rhino sinusitis as well as a good understanding of the relationship of the anatomical structures in the nasal cavity.

Key words: Cavalieri's principle, volume analysis, micro-computed tomography, New Zealand white rabbit, paranasal sinus, concha, meatus

Introduction

The relationship between the structures in the nasal cavity is important for many fields [19]. At the same time, the variety and proximity of the anatomical relationships of structures in this region and its surroundings (such as brain cavity, paranasal sinus) should be well known for approaches such as paranasal sinus surgery, functional endoscopic sinus surgery, treatment choices, simulations, and planning [18, 19, 23]. The rabbit model is used for such purposes [5, 12, 22]. Imaging techniques such as computerized tomography are used to determine structures and monitor changes for experimental or diagnostic purposes on chronic rhino sinusitis, sinusitis, paranasal sinus pathologies, and obstruction on these models [4, 6, 12, 20]. However, it is very important to know normal anatomy for the evaluation of the images obtained from imaging techniques [21].

No matter how complicated it is, the 3D rendering process generated from images obtained from imaging techniques has been made easier to understand the positions, relationships, morphometric measurements and forms of anatomical structures. The most important reason for this complexity is that the regions of anatomical structures should be well known [2, 10, 19]. Especially the detail created by μCT in bone tissue is used to distinguish between anatomical structures [5, 11]. The quality of education can be increased, more realistic observations can be made, patient-specific approaches can be applied and new plans can be created with these 3D models [6, 10, 18, 23].

Rabbits are preferred in experimental studies as the volume of the nasal cavity is similar to human [5, 17, 22]. The volume estimation for the examination of paranasal sinuses is an easily determinable but highly important index [18, 19, 20]. Although the determination of the volumetric data of the structures belonging to this region has been done with different imaging techniques and methodologies [16, 22], no study has been found in the Cavalieri principle, which is considered as the gold standard for volume estimation for the past decade. Efficient and unbiased volumetric estimations are made by Cavalieri's principle on macroscopic [9], histological [1, 3] and MRI or CT images [13, 14, 18].

Therefore, this study aims to evaluate the relationships of the rabbit nasal cavity by using a high definition μCT images with 3D reconstruction models for the more accurate understanding and to estimate and compare the volume measurements of the structures in and surrounding area by Cavalieri's principle and manual segmentation.

Materials and Methods

Five adult male (1-year-old / 3000-3500 g) New Zealand white rabbits that were prepared for the educational reasons were used in the study. This study was confirmed by Ankara University Animal Experiments Local Ethics Committee (Decision no. 2019-3-19). Rabbit craniums were dissected from surrounding tissues and divided into two from the midpoint. Then, they were imaged with the μCT device (Super Argus PET / CT, Sedecal, Spain). Image processing was performed at standard resolution, 0.12 mm slice thickness, 40 kV and 140 μA. Cross-section images were uploaded to the 3D Slicer software program (3D slicer, 4.11.0 version, GitHub, San Francisco) for segmentation. During the segmentation process, the "segment editor" function was used to separate all tissues from each other. Manual segmentation was performed inside the cavities. 3D reconstruction models of the MS, DCS, VNC, MNC, VNM, MNM, DNM, NV, and CC were applied for volume analysis and visualization of the tissues. Different colors were selected for segmentation of these regions (Fig. 1). Then, the "segmentation statistics" function was used for the volume estimations of these 3D models.

On the other hand, μCT image series were used to estimate volume values of each part of the cavities by using the Cavalieri's principle (Fig. 2). Volume estimations were performed using the Cavalieri probe of the Stereo Investigator Software (Version 10.50, MBF Bioscience, USA). In accordance with the systematic random sampling, one of ten were selected for each μCT images series of CC, MS, DCS, DNM, MNM, VNM, and VNC and one of two were selected for NV. The distance between two points assigned by point counting grid for each section was determined as 1500 µm. The volume calculations were carried out by the following formula:

$V = Ap \times m \times t \times (\sum P)$

where: V- volume of the focused region; m- section evaluation range; Ap- is the area of each point on the point counting grid; t- is cross section thickness and; P- is the number of points at the desired region in sections. The coefficient of error (CE) for every region was calculated by the software in order to see the reliability of the CP [7, 8].

Two determinant was used to compare the results of manual segmentation and the Cavalieri's principle: a) volumes and b) volumetric analysis time. Descriptive statistics were calculated for each variable. Before hypothesis testing differences of each pair were evaluated for normality using Shapiro Wilk test. Paired sample t-test was used to evaluate the difference between stereological and 3D measurements. Bland Altman plot was used to describe the agreement between stereology and 3D measurements by constructing limits of agreement. A probability value of less than 0.05 was considered significant. SPSS v21 statistical software was used for data analysis.

Results

The 3D reconstructed models of the rabbit nasal regions and cranial cavity were displayed in Figure 1. Four different transversal cross-sections were presented with % 50 transparency from VNC level at 7.603 mm (Fig. 1-D), DCS level at 22.171 mm (Fig. 1-C), end of the nasal cavity level at 38.171 mm (Fig. 1-B) and approximately end of the brain hemisphere level at 76.266 mm (Fig. 1-A).

Four transverse cross-section images, at which 3D rendering and their corresponding Cavalieri principle volume estimation sections, were given in Figure 2. Statistical differences between the volume measurements of CC, MS, DCS, DNM, MNM, VNM, VNC, MNC, and NV of two methods were estimated and given in Table 1. There was a statistically significant difference between methods of the MS, DCS, DNM, MNM, VNM, VNC, and MNC volume measurements ($P<0.001$). On the other hand, the time period of both methods was recorded and compared. The time period for each step was given in Table 2. There was a statistically significant difference between the volumetric analysis time period of the methods and Cavalieri's principle was found much shorter than manual segmentation.

The average agreement between Stereology and 3D measurements were shown in Table 3 and Figure 3. On average, Stereology method was measured 112.3 units more than 3D method. Only the NV was the closest to ideal. This positive bias was seen to be due to measurements over 400, while for lower concentrations data were closer to each other.

Discussion

The anatomy, morphometry, and relationship of the structures in the nasal cavity have attracted the attention of many researchers such as anatomists, radiologists, surgeons or otolaryngologists [5, 6, 10, 16]. It was determined that the composed 3D reconstruction models by μCT images provided a preferable anatomical approach to the nasal cavity structures for the visual aspect. Methodological outcomes of this study proved that the Cavalieri's principle was determined as an efficient and objective volume estimation method than the manual segmentation. It was seen that manual segmentation of 3D rendering was a time-consuming approach to calculate volumetric values. The reliability property makes the Stereology methodologies valuable and superior.

Pirner et al. [18] stated that the anatomy of the nasal cavity was very complex so the differentiation of the region borders was difficult. In this case, they were emphasized that semi-automatic segmentation was limited. On the other hand, it was indicated that CT scans and manual segmentation were determined as a gold standard for the evaluation of the paranasal sinuses [10]. μCT cross-section images were easily applied to the volume calculation procedures on both methods because of having a high resolution of tissues in this study. As noted in previous studies, this convenience comes from the high resolution of μCT [5, 11, 17, 21]. On the other hand, as reported in a previous study [18], it was observed that 3D reconstruction models and 2D images of the μCT of the nasal cavities were observed to be useful educational materials for students, researchers, radiologist or surgeons who work in this field. According to the literature and this study, DCS was found above the MS. These sinuses were opened to each other with a deep hole and communicated with the nasal cavity by a narrow hole

[5]. The frontal sinus was not observed in this study. This result was consistent with the previous studies [5, 16]. The sphenoidal sinus was not also observed in this study. This result was consistent with the previous study [16].

The volume analysis time of the 3D reconstruction method was significantly higher than the Cavalieri's principle in this study. It was indicated that the manual segmentation of the nasal cavity and paranasal sinuses took 8-10 hour for one CT dataset of a human [6, 18]. In another study, the total time of the manual and semi-automatic segmentation of the paranasal sinuses were calculated 980 and 765 minutes, respectively [19]. It was also seen that semi-automated segmentation of a horse paranasal sinus took approximately 8-12 hour [2]. The total time duration of the manual segmentation was seen four times higher than the Cavalieri's principle in this study. In addition to that, the image optimization and sampling standardization steps are performed once for a tissue or organ in the Cavalieri's principle. So these steps only take time once. This situation is reduced elapsed time very much. An unconstrained smoothing was used to overcome the rough surface problem in the correction stage on 3D models. It was also preferred by some previous studies [2, 19].

In previous studies, it was mentioned that the volume parameter is the most valuable and important index [10, 17, 18]. The volume of the anterior and posterior MS was determined 0.6 and 0.7 in the mouse, 8.6 and 7.7 in the rat, and 63.5 and 46.6 mm^3 in the guinea pig, respectively [17]. The mean volume values of the MS, VNC, MNC, and DNC have been calculated to range from 817.53 ± 86.71, 534.15 ± 95.78, 435 ± 81.7 and 262.87 ± 74.06 mm^3 in a previous study, respectively [16]. The result of the MS and DNC volume of this study was consistent with these in the previous study [16] but VNC and MNC volumes were different from the same study.

No stereological study, particularly about the nasal cavity region, was found as the similar content with our research. Furthermore, Bland Altman is used for concordance instead of correlation analysis in this study. Agreement for the two methods was summarized in terms of 'limits of agreement', which involves an examination of the variability of the differences, since the correlation between methods is always misleading and should not be used for assessing the method comparability [15]. In this study, it was observed that the correlation was high in the regions where the boundaries were clearly determined, but the differences increased in the regions with complex boundaries. It was thought that this situation is made important the selection of the anatomical structure, the researcher, and the method for the estimation and evaluation of the measurement results.

Conclusions

Although morphometric measurements of the nasal and cranial cavity estimated in the previous studies, this study gave unbiased, precise and efficient estimations of these regions with Cavalieri's principle. μCT is a superior imaging technique for scanning the complex and tiny anatomical structures. In addition to that, μCT images can be preferable for creating detailed 3D reconstruction models. For future planning, first of all, age-related volumetric differences should be examined. Quantitative and anatomical changes of the nasal cavity structures can be compared in the direction of the advancing age. Secondly, 3D printing models could also be produced for anatomy training. In this way, in addition to 2D and 3D images, a new educational approach could be given to students.

Acknowledgments

The authors would like to thank Dr. Doğukan Özen from the Department of Biostatistics, Faculty of Veterinary Medicine, Ankara University for performing the statistical analysis.

References

1. Bakici C, Oto Ç, Ekim O, et al. Comparison of the volume fraction values of grey matter on the cervical enlargement of the spinal cord in chicken and quail. Ankara Univ Vet Fak Derg. 2019; 66(1): 1-6. doi: 10.1501/Vetfak_0000002880.
2. Brinkschulte M, Bienert-Zeit A, Lüpke M et al. Using semi-automated segmentation of computed tomography datasets for three-dimensional visualization and volume measurements of equine paranasal sinuses. Vet Radiol Ultrasound. 2013; 54(6): 582-590. doi: 10.1111/vru.12080, indexed in Pubmed: 23890087.
3. Cakmak G, Karadag H. A morphological and stereological study on calculating volume values of thoracic segments of geese. Folia Morphol. 2019; 78(1): 145-152. doi: 10.5603/FM.a2018.0115, indexed in Pubmed: 30543082.

4. Capello V. Rhinostomy as Surgical Treatment of Odontogenic Rhinitis in Three Pet Rabbits. J Exot Pet Med. 2014; 23(2): 172-187. doi: 10.1053/j.jepm.2014.02.005.
5. Casteleyn C, Cornillie P, Hermens A, et al. Topography of the rabbit paranasal sinuses as a prerequisite to model human sinusitis. Rhinology. 2010; 48(3): 300-304. doi: 10.4193/Rhin09.193, indexed in Pubmed: 21038020.
6. Cherobin GB, Voegels RL, Gebrim EMMS, et al. Sensitivity of nasal airflow variables computed via computational fluid dynamics to the computed tomography segmentation threshold. PLoS One. 2018; 13(11): e0207178. doi: 10.1371/journal.pone.0207178, indexed in Pubmed: 30444909.
7. Garcia-Finana M, Cruz-Orive LM, Mackay CE, et al. Comparison of MR imaging against physical sectioning to estimate the volume of human cerebral compartments. Neuroimage. 2003; 18(2): 505-516. doi: 10.1016/S1053-8119(02)00021-6, indexed in Pubmed: 12595203.
8. Gundersen HJG, Jensen EB. The efficiency of systematic sampling in stereology and its prediction. J Microsc. 1987; 147(3): 229-263. doi: 10.1111/j.1365-2818.1987.tb02837.x, indexed in Pubmed: 3430576.
9. Ince NG, Pazvant G, Onar V, et al. Volume calculation of the cattle (Bos taurus L.) and the water buffalo (Bos bubalis L.) metapodia with stereologic method. Folia Morphol. 2015; 74(3): 335-339. doi: 10.5603/FM.2015.0050, indexed in Pubmed: 26339814.
10. Kapakin S. The paranasal sinuses: three-dimensional reconstruction, photo-realistic imaging, and virtual endoscopy. Folia Morphol. 2016; 75(3): 326-333. doi: 10.5603/FM.a2016.0006, indexed in Pubmed: 26916200.
11. Kozerska M, Skrzat J. Anatomy of the fundus of the internal acoustic meatus - micro-computed tomography study. Folia Morphol. 2015; 74(3): 352-358. doi: 10.5603/FM.2015.0053, indexed in Pubmed: 26339817.
12. Lennox AM. Rhinotomy and rhinostomy for surgical treatment of chronic rhinitis in two rabbits. J Exot Pet Med. 2013; 22(4): 383-392. doi: 10.1053/j.jepm.2013.10.001.
13. Marino MJ, Riley CA, Kessler RH et al. Clinician assessment of paranasal sinus pneumatization is correlated with total sinus volume. Int Forum Allergy Rhinol. 2016; 6(10): 1088-1093. doi: 10.1002/alr.21779, indexed in Pubmed: 27159784.
14. Oto C, Bakici C, Tunca M, et al. Stereological estimation of volume ratios of chest

muscle in Atak-s hybrid with Rhode Island Red and Barred Rock pure lines by magnetic resonance imaging. Vet Hekim Der Derg. 2017; 88(2): 3-14.
15. Ozen D. Evaluation of concordance between measurement techniques using graphical methods and regression models with an application. Eurasian J Vet Sci, 2018; 34(4): 265-271. doi: 10.15312/EurasianJVetSci.2018.209.
16. Ozkadif S, Eken E. Three-dimensional reconstruction of multidetector computed tomography images of paranasal sinuses of New Zealand rabbits. Turk J Vet Anim Sci. 2013; 37(6): 675-681. doi:10.3906/vet-1301-53.
17. Phillips JE, Ji L, Rivelli MA, et al. Three-dimensional analysis of rodent paranasal sinus cavities from X-ray computed tomography (CT) scans. Can J Vet Res. 2009; 73(3): 205-211. indexed in Pubmed: 19794893.
18. Pirner S, Tingelhoff K, Wagner I, et al. CT-based manual segmentation and evaluation of paranasal sinuses. Eur Arch Otorhinolaryngol. 2009; 266: 507-518. doi: 10.1007/s00405-008-0777-7, indexed in Pubmed: 18716789.
19. Tingelhoff K, Moral AI, Kunkel ME, et al. Comparison between manual and semi-automatic segmentation of nasal cavity and paranasal sinuses from CT images. Conf Proc IEEE Eng Med Biol Soc. 2007; 2007: 5505-5058. doi: 10.1109/IEMBS.2007.4353592, indexed in Pubmed: 18003258.
20. Valtonen O, Bizaki A, Kivekas I, et al. Three-dimensional volumetric evaluation of the maxillary sinuses in chronic rhinosinusitis surgery. Ann Otol Rhinol Laryngol. 2018; 127(12): 931-936. doi: 10.1177/0003489418801386, indexed in Pubmed: 30244583.
21. Van Caelenberg AI, De Rycke LM, Hermans K et al. Computed tomography and cross-sectional anatomy of the head in healthy rabbits. Am J Vet Res. 2010; 71(3): 293-303. doi: 10.2460/ajvr.71.3.293, indexed in Pubmed: 20187831.
22. Xi J, Si XA, Kim J, et al. Anatomical details of the rabbit nasal passages and their ımplications in breathing, air conditioning, and olfaction. Anat Rec. 2016; 299(7): 853-868. doi: 10.1002/ar.23367. Epub 2016 May 17, indexed in Pubmed: 27145450.
23. Zhang XD, Li ZH, Wu ZS et al. A novel three-dimensional-printed paranasal sinus-skull base anatomical model. Eur Arch Otorhinolaryngol. 2018; 275(8): 2045-2049. doi: 10.1007/s00405-018-5051-z29959564, indexed in Pubmed: 29959564.

Table 1. Statistical parameters of the nasal and cranial cavity regions and volume indexes divided for method groups. The values are presented in mm^3.

Region	Mean	SEM	SD	Median	Min	Max	P	CE
MS CP	678.2	4.49	14.21	680.61	660.11	696.11	<0.001	0.02
MS 3D	867.69	11.09	35.08	875.07	815.46	907.19		0.02
DCS CP	229.01	0.87	2.76	229.9	224.13	232.46	<0.001	0.04
DCS 3D	310.41	1.22	3.85	310.4	305.24	317.03		0.04
VNC CP	291.01	3.08	9.76	293.44	278.16	305.27	<0.001	0.04
VNC 3D	311.79	2.67	8.45	309.18	301.95	324.89		0.04
MNC CP	367.28	4.22	13.36	374.23	345.13	380.57	<0.001	0.05
MNC 3D	233.19	5.85	18.5	241.18	200.16	250.52		0.05
VNM CP	57.5	0.43	1.35	57.33	55.29	59.63	<0.001	0.06
VNM 3D	147.57	1.99	6.29	145.14	140.23	160.95		0.06
MNM CP	232.06	1.51	4.78	231.5	224.92	240.16	<0.001	0.02
MNM 3D	774.13	5.27	16.67	777.41	750.12	795.29		0.02
DNM CP	80.52	0.68	2.16	81.21	75.65	83.34	<0.001	0.05
DNM 3D	189.5	1.88	5.95	189.91	179.43	199.16		0.05
NV CP	66.19	0.45	1.41	66.24	63.22	67.98	0.983	0.2
NV 3D	66.17	0.82	2.59	66.08	60.23	69.42		0.2
CC CP	11556	190.77	426.56	11450.12	11103.5	12120.14	0.42	0.003
CC 3D	11337.21	81.76	182.81	11366	11099.89	11557.03		0.003
Time CP	475.8	6.83	15.27	475	461	501	<0.001	-
Time 3D	136.6	1.4	313	138	132	140		-

Abbreviations – see text.

Table 2. Volume analysis time for each step of two methods. The values are presented in minutes.

Procedure	Step	Time

3D reconstruction	μCT	30
	Segmentation	375.6
	Correction	60
	3D modeling	9.2
	Quantitative estimation	1
	Total	475.8*
Cavalieri principle	μCT	30
	Image optimization	1
	Sampling standardization	30
	Quantitative estimation	66.6
	Total	136.6*

* An asterisk indicates a significant difference between groups within the same column ($P < 0.001$).

Table 3. Agreement between Stereology and 3D methods.

Area	Bias Estimate	Lower	Upper
		Limit of Agreement	
MS	189.492	110.788	268.196
DCS	81.403	74.219	88.587
VNC	20.786	6.400	35.172
MNC	-134.092	-189.453	-78.731
VNM	90.066	78.895	101.238
MNM	542.062	511.654	572.470
DNM	108.980	98.539	119.420
NV	-0.023	-6.583	6.538
CC	-218.786	-1.286.317	848.745
All areas*	112.334	-254.232	478.901

*Cranial cavity is excluded. Abbreviations – see text.

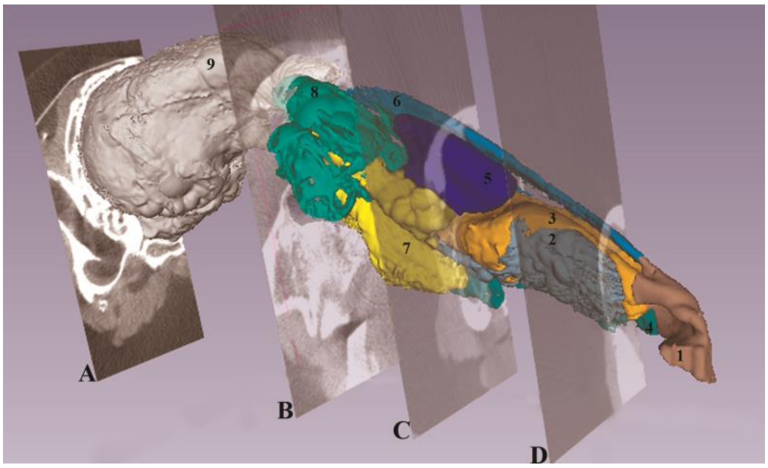

Figure 1. 3D reconstruction models of the nasal and cranial cavity regions by using the µCT. Scanning planes are perpendicular to the nasal septum; A- end of the brain hemisphere, B- End of the nasal cavity level, C- DCS level and D- VNC level. 1- NV, 2- VNC, 3- MNM, 4- VNM, 5- DCS, 6- DNM, 7- MS, 8- MNC, and 9- CC.

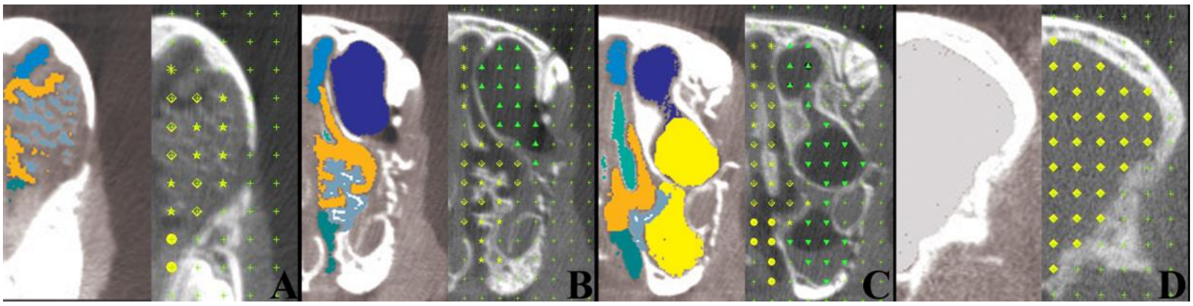

Figure 2. Images of the volume estimation of the Cavalieri's principle (right) its corresponding µCT 3D rendering images (left) (A-D).

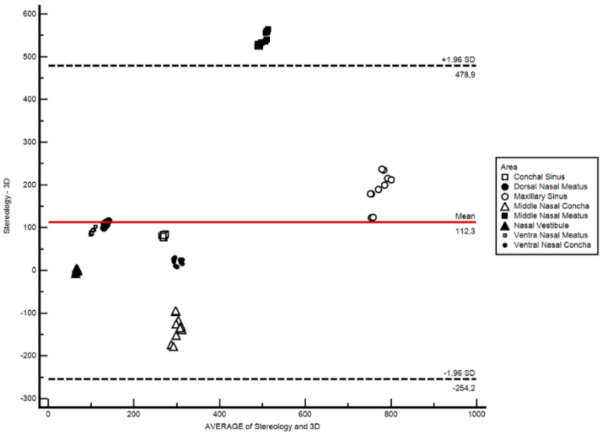

Figure 3. The plot of differences between Stereology and 3D versus the mean of the two measurements. The bias of 112.3 units is represented by the parallel red line at 112.3 units.